Supplementary materials

1. Characterization of the $NiFe_2O_4$

As shown in inset of Supplementary Fig. 1, SEM image displays the morphology of $NiFe_2O_4$. Clearly, $NiFe_2O_4$ was formed with irregular shapes of 50-100 nm in diameter, which was smaller than those (~ 250 nm) in previous report [22]. At the same time, the as-synthesized $NiFe_2O_4$ MNPs were rugged and more likely to be agglomerated. This condition was unavoidable as their strong superparamagnetism led to magnetic interactions. The large amount of gaps showed the prominent advantage with high adsorption capacity for magnetic enrichment of analytes (inset of Supplementary Fig. 1a).

The crystalline phase of $NiFe_2O_4$ MNPs was analyzed by XRD patterns (Supplementary Fig. 1a). The diffraction peaks of as-synthesized samples matched well with the Jade PDF card for simulated $NiFe_2O_4$ in the range of 20-70° (JCPDS 10-325) and no more impurity peaks were observed. The peaks were obvious and sharp, reflecting the good crystallinity of the sample. It was in full agreement with the previous literature [26], which indicated the successful synthesis of $NiFe_2O_4$ MNPs.

The N_2 sorption-desorption isotherms showed that the BET surface area was 14.1 $m^2\ g^{-1}$, which was much larger than that (9.6 $m^2\ g^{-1}$) of commercial Fe_3O_4, thereby contributing the higher adsorption efficiency. Sufficient magnetism contributed to effectively and quickly recover MNPs containing analytes. By means of a vibrating sample magnetometer (VSM), and the magnetization curves on magnetic adsorbent are shown in Supplementary Fig. 1b before and after adsorption of metal ions. The value of specific saturation magnetization (M_s) was 38.9 emu g^{-1} before adsorption, while it tailed off to 36.9 emu g^{-1} after adsoption of metal ions. And the drop in *Ms* values

possibly resulted from the increase of adsorption of metal ions on the surface of $NiFe_2O_4$. The insert image proved that $NiFe_2O_4$ could be well dispersed and distributed in aqueous solution, and sank into the bottom using an external magnet. A fast and facile separation process of metal ions with magnetic $NiFe_2O_4$ was also demonstrated in the image (inset of Supplementary Fig. 1b).

The functional groups of $NiFe_2O_4$ were analyzed using FT-IR spectra (Supplementary Fig. 1c). The obvious absorption peaks at 418.2 cm^{-1} and 601.6 cm^{-1} were assigned to the stretching vibrations of Fe-O and Ni-O [1], and the bands at 3445.9 cm^{-1} stretching vibrations was related to O-H which showed the presence of water molecules. The band near 1624.8 cm^{-1} was attributed to carboxyl (C=O) stretching vibration [26]. Additionally, the peaks of oxygen-containing functional groups exhibited a slight shift to lower frequency after adsorption of metal ions adsorption such as the hydroxyl (OH) and C=O groups with slight shifts from 3445.9 to 3447.6 cm^{-1} and from 1624.8 to 1625.6 cm^{-1}, respectively. The presence of C=O and -OH contributed to occurrence of a higher adsorption efficiency between $NiFe_2O_4$ and metal ions. As a result, it could be inferred from the shifting and weakening in intensity of bands that the functional groups and electrostatic attraction played an important role in interaction between metal ions and $NiFe_2O_4$.

Supplementary References

1- R.D. Waldron, Phys. Rev., 1955, **99**, 1727-1735.

Supplementary Table 1. The operating conditions of Agilent 8800 ICP-MS instrumentation

RF power (W)	1400
Sample flow rate (mL min^{-1})	0.5
Nebulizer type	Mira Mist
Spray chamber	Scott-type double pass
Gas flow rates (L min^{-1})	Plasma, 15; auxiliary, 1.2; nebulizer, 0.8
Collision Gas: He	Flow: 4.5 mL min^{-1}
Spectrum Mode	Q2 Peak Pattern: 1 Point
Sampler cone	Ni, 1.0 mm
Skimmer cone	Ni, 0.8 mm
Dwell time (ms)	30 in standard mode
Replicates	3

Supplementary Table 2. Intra-day and inter-day precision of the proposed MNET-DSPM/ICP-MS method

Analytes	Intra-day precision (RSD%, n=6)			Inter-day precision (RSD%, n=6)		
	Low	Medium	High	Low	Medium	High
Mn	5.4	4.4	3.1	6.1	5.9	4.2
Cu	4.9	3.2	2.4	4.5	4.1	3.7
Zn	4.2	4.0	2.7	5.5	5.1	4.2
Cd	5.3	5.0	1.5	4.2	3.7	2.8

Note: (1) "high" indicates 100 μg kg^{-1} for seafoods; (2) "medium" indicates 20 μg kg^{-1} for seafoods; (3) "low" indicates 2.0 μg kg^{-1} for seafoods.

Supplementary Table 3. Analysis of certified reference materials (n=3)

Samples	Certified value				Found				Recovery (%)			
	Cd	Cu	Zn	Mn	Cd	Cu	Zn	Mn	Cd	Cu	Zn	Mn
GBW10024	1.06	1.34	75	19.2	1.01	1.30	72.8	18.9	95.2	97.0	97.1	98.4
(μg/g)/Shellfish	±0.10	±0.18	±3	±1.2	±0.07	±0.02	±2.1	±0.8				
GBW10050	0.03	10.3	76	8.9	0.029	9.83	73.5	8.6	96.7	95.4	96.7	96.6
(μg/g)/Shrimp	±0.002	±0.7	±4	±0.3	±0.01	±0.4	±3.8	±0.2				

Supplementary Fig. 1

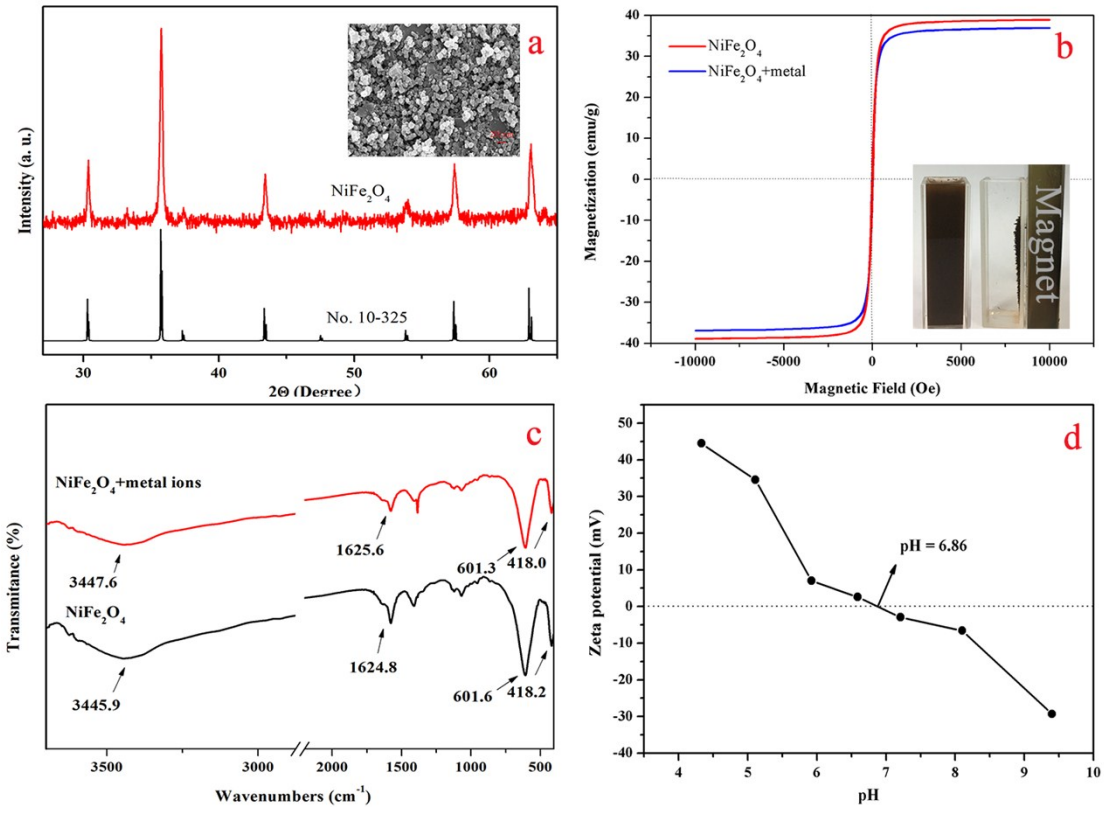

Supplementary Fig. 2

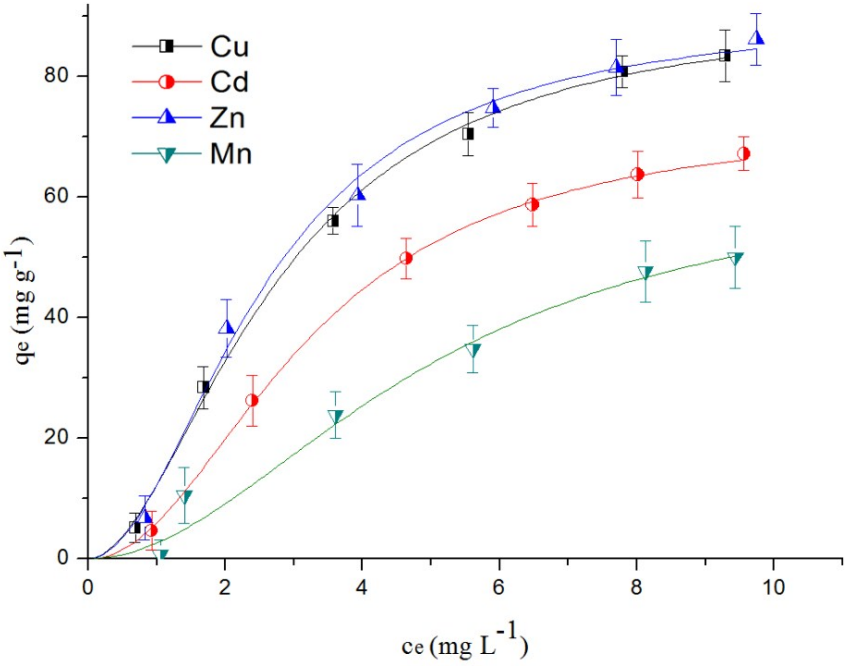

Supplementary Fig. 3